PM/95-20
THES-TP 95/07
May 1995

Anomalous Couplings in Single Higgs Production through $\gamma\gamma$ Collisions [1]

G.J. Gounaris[a] and F.M. Renard[b]

[a]Department of Theoretical Physics, University of Thessaloniki,
Gr-54006, Thessaloniki, Greece,

[b]Physique Mathématique et Théorique, CNRS-URA 768,
Université de Montpellier II, F-34095 Montpellier Cedex 5.

Abstract

We show that single Higgs production in $\gamma\gamma$ collisions through laser backscattering provides the best way to look for New Physics (NP) effects inducing anomalous Higgs couplings. Our analysis is based on the four $dim = 6$ operators $\mathcal{O}_{UB}$, $\mathcal{O}_{UW}$, $\overline{\mathcal{O}}_{UB}$ and $\overline{\mathcal{O}}_{UW}$ which describe New Physics effects in this sector. Using the Higgs production rate we establish observability limits for the couplings of the aforementioned operators at a level of 10^{-3}, which means establishing lower bounds on the scale of NP of the order 30 to 200 TeV. Higgs branching ratios, especially the ratio $\Gamma(H \to \gamma\gamma)/\Gamma(H \to \gamma Z)$, are shown to provide powerful ways to disentangle the effects of the various operators.

[1]Partially supported by the EC contract CHRX-CT94-0579.

1 Introduction

Future high energy linear e^+e^- colliders should allow the realization of $\gamma\gamma$ collisions with intense high energy photon beams through the laser backscattering method [1]. Provided the Higgs particle will be accessible at the future colliders, the $\gamma\gamma$ fusion into a single Higgs boson has been recognized as being a powerful tool to study the anomalous Higgs couplings and thereby the scalar sector of the electroweak interactions [2]. These anomalous Higgs couplings may arise as residual effects of a New Physics (NP) characterized by a scale $\Lambda \gg M_W$.

It has been shown that there exist seven $dim = 6$ $SU(2) \times U(1)$ gauge invariant operators which are not strongly constrained by existing LEP1 experiments and provide a reasonably complete description of the residual purely bosonic NP interactions at energies lower than Λ [3, 4, 5, 6]. Furthermore, only four of these operators dubbed $\mathcal{O}_{UB}$, $\mathcal{O}_{UW}$, $\overline{\mathcal{O}}_{UB}$ and $\overline{\mathcal{O}}_{UW}$, create Higgs anomalous couplings exclusively and are therefore not affected by constraints on the anomalous gauge couplings. A first study of the operator $\mathcal{O}_{UW}$ has already been done in [7] by looking into vector boson production through $\gamma\gamma$ collisions, and subsequently in [2] where $\gamma\gamma \to H$ and the various Higgs branching ratios have been analysed.

In the companion paper [8] we have presented a complete analysis of what can be learned for all seven operators by using weak boson pair production at $\gamma\gamma$ colliders. The aim of the present paper is to perform an analysis of the process $\gamma\gamma \to H$ and of the Higgs decay modes. These later processes are particularly sensitive to $\mathcal{O}_{UB}$, $\mathcal{O}_{UW}$, $\overline{\mathcal{O}}_{UB}$, $\overline{\mathcal{O}}_{UW}$ and can be used to strongly constrain their couplings.

The Standard contribution to $\gamma\gamma \to H$ only occurs at 1-loop. With the high luminosities expected at linear e^+e^- colliders, a large number of Higgs bosons should be produced. The sensitivity to anomalous $H\gamma\gamma$ couplings is therefore very strong. It turns out that $\gamma\gamma \to H$ can be used to put an observability limit of the order of 10^{-3} on these couplings, which means that NP scales of up to several tens of TeV can be probed. This range largely covers the domain of characteristic scales expected by several theoretical models.

The disentangling of the four operators $\mathcal{O}_{UB}$, $\mathcal{O}_{UW}$, $\overline{\mathcal{O}}_{UB}$ and $\overline{\mathcal{O}}_{UW}$ is further helped by considering the Higgs decay branching ratios. Concerning this we remark that $H \to b\bar{b}$ is not affected by the aforementioned seven purely bosonic operators descibing NP. Neither $H \to WW$, ZZ are particularly sensitive to such an NP, since it is masked by strong tree level SM contributions. On the other hand, the processes $H \to \gamma\gamma$ and $H \to \gamma Z$ who receive tree level contributions from the above anomalous couplings and only one loop ones from SM, are most sensitive to NP. Thus their ratio to the dominant Higgs decay mode, which depending on the Higgs mass may either be the $b\bar{b}$ or the WW, ZZ modes, provide a very sensitive way to further help disentangling among the CP conserving operators $\mathcal{O}_{UB}$ and $\mathcal{O}_{UW}$. This way, using $H \to \gamma\gamma$ or $H \to \gamma Z$, couplings even weaker than 10^{-3} could be observable. For comparison we note that the corresponding sensitivity limit from $H \to WW$, ZZ is at the 10% level. The identification of the CP-violation effects and the disentangling of the CP-violating operators from the CP-conserving ones requires a study of either the W,Z spin density matrix through their decay distributions or of initial $\gamma\gamma$

linear polarization effects.

In Section 2 we give the explicit expression of the production rate of Higgs through $\gamma\gamma$ collisions at a linear collider, including SM and NP contributions due to the four operators. We consider collider energies of 0.5, 1 and 2 TeV. Section 3 is devoted to the study of the Higgs decay modes $H \to \gamma\gamma$, γZ, WW, ZZ, $b\bar{b}$ and to the computation of the SM and NP effects for the various ratios. A discussion of the sensitivities to the anomalous couplings and of the possibility to disentangle the contributions from the various operators is given in Section 4.

2 The $\gamma\gamma \to H$ production rate

The formalism of $\gamma\gamma$ collisions through laser backscattering has been described in [1]. We shall use the same notations as in [2]. The cross section for $\gamma\gamma \to H$ is given by

$$\sigma = \mathcal{L}_{\gamma\gamma}(\tau_H) \left(\frac{8\pi^2}{m_H}\right) \frac{\Gamma(H \to \gamma\gamma)}{s_{ee}} \quad , \tag{1}$$

where the luminosity function $\mathcal{L}_{\gamma\gamma}(\tau_H)$ for $\tau_H = m_H^2/s_{ee}$ is explicitly given in terms of the $f_{\gamma/e}^{laser}$ distribution in [2, 7]. Essentially $\mathcal{L}_{\gamma\gamma}$ is close to the e^+e^- linear collider luminosity $\mathcal{L}_{ee}$ up to $\tau_{max} = (0.82)^2$.

The $H \to \gamma\gamma$ decay width is computed in terms of the one-loop SM contribution and tree level NP ones [9]:

$$\Gamma(H \to \gamma\gamma) = \frac{\sqrt{2}G_F}{16\pi} m_H^3 \left(\left| \frac{\alpha}{4\pi} (\frac{4}{3} F_t + F_W) - 2ds_W^2 - 2d_B c_W^2 \right|^2 + 4|\bar{d}s_W^2 + \bar{d}_B c_W^2|^2 \right) \ , \tag{2}$$

where the standard top and W contributions are respectively determined by

$$F_t = -2t_t(1 + (1 - t_t)f(t_t)) \quad , \tag{3}$$

$$F_W = 2 + 3t_W + 3t_W(2 - t_W)f(t_W)) \quad , \tag{4}$$

in terms of

$$f(t) = \left[sin^{-1}(1/\sqrt{t}) \right]^2 \qquad \text{if} \quad t \geq 1 \quad ,$$

$$f(t) = -\frac{1}{4} \left[\ln \left(\frac{1 + \sqrt{1-t}}{1 - \sqrt{1-t}} \right) - i\pi \right]^2 \qquad \text{if} \quad t < 1 \quad , \tag{5}$$

with $t_t = 4m_t^2/m_H^2$, $t_W = 4M_W^2/m_H^2$ and $m_t = 175GeV$ [10]. The NP contributions are obtained from the Lagrangian given in eqs. (8) in the companion paper, where also the definitions of the various operators are given.

The resulting rate is shown in Fig.1-2 for three typical NLC energies, 0.5, 1 and 2 TeV. The number of events indicated in these figures corresponds to e^+e^- luminosities of 20, 80

and 320 fb^{-1} respectively. Strong interference effects may appear (depending on the Higgs mass) between the SM and the CP-conserving NP contributions; (compare Fig.1). But in the case of CP-violating contributions (Fig.2) there are never such interferences. In the figures we have only illustrated the cases of $\mathcal{O}_{UW}$ and $\overline{\mathcal{O}}_{UW}$. The corresponding results for $\mathcal{O}_{UB}$ and $\overline{\mathcal{O}}_{UB}$ can be deduced according to eq(2) from Fig.1-2, by the replacement $d\,[\bar{d}] \to c_W^2/s_W^2 d_B\,[\bar{d}_B]$. So the sensitivity to these last two operators is enhanced by more than a factor 3 in the cross section.

With the aforementioned designed luminosities, one gets a few thousands of Higgs bosons produced in the light or intermediate mass range. Assuming conservatively an experimental detection accuracy of about 10% on the production rate, one still gets an observability limit of the order of 10^{-3}, 4.10^{-3}, 3.10^{-4}, 10^{-3} for d, $\bar{d}$, d_B and $\bar{d}_B$ respectively. The corresponding constraints on the NP scale derived on the basis of the unitarity relations [11, 12, 5], are 200, 60, 60 and 30 TeV respectively.

3 Higgs decay widths and ratios

The expression of the $H \to \gamma\gamma$ width has been written above in (2). Correspondingly, the $H \to \gamma Z$ width is also expressed in terms of a 1-loop SM contribution and of the NP contributions from the four operators [9]:

$$\Gamma(H \to \gamma Z) = \frac{\sqrt{2}G_F m_H^3}{8\pi}\Big(1-\frac{M_Z^2}{m_H^2}\Big)^3\left(\Big|\frac{\alpha}{4\pi}(A_t+A_W)+2(d-d_B)s_W c_W\Big|^2 + 4s_W^2 c_W^2|\bar{d}-\bar{d}_B|^2\right), \quad (6)$$

$$A_t = \frac{(-6+16s_W^2)}{3s_W c_W}[I_1(t_f,l_t)-I_2(t_t,l_t)] \quad , \quad (7)$$

$$A_W = -cot\theta_W[4(3-tan^2\theta_W)I_2(t_W,l_W)+[(1+\frac{2}{t_W})tan^2\theta_W-(5+\frac{2}{t_W})]I_1(t_W,l_W)] \ , \quad (8)$$

where $t_t = 4m_t^2/m_H^2$, $t_W = 4M_W^2/m_H^2$ as before, and $l_t = 4m_t^2/M_Z^2$, $l_W = 4M_W^2/M_Z^2$. In (7, 8) the definitions[1]

$$I_1(a,b) = \frac{ab}{2(a-b)} + \frac{a^2b^2}{2(a-b)^2}[f(a)-f(b)] + \frac{a^2b}{(a-b)^2}[g(a)-g(b)] \ , \quad (9)$$

$$I_2(a,b) = -\frac{ab}{2(a-b)}[f(a)-f(b)] \quad , \quad (10)$$

[1]There is a discrepancy in the relative sign of the $g(x)$ and $f(x)$ terms between the first paper in [9] and the remaining two. Here we follow the results of the later two papers.

where $f(t)$ is given in (5) and

$$g(t) = \sqrt{t-1} sin^{-1}(\frac{1}{\sqrt{t}}) \qquad \text{if} \qquad t \geq 1 \quad ,$$

$$g(t) = \frac{1}{2}\sqrt{1-t}\left[ln\left(\frac{1+\sqrt{1-t}}{1-\sqrt{1-t}}\right) - i\pi\right] \qquad \text{if} \qquad t < 1 \quad . \tag{11}$$

The $H \to W^+W^-, ZZ$ widths receive a tree level SM contribution which interfere with the ones from the CP-conserving operators $\mathcal{O}_{UB}, \mathcal{O}_{UW}$. In addition there exist quadratic contributions from the CP-violating operators $\overline{\mathcal{O}}_{UB}$, $\overline{\mathcal{O}}_{UW}$. For $m_H > 2M_V$, $V = W, Z$ one gets

$$\begin{aligned}\Gamma(H \to VV) &= C_V \left(\frac{\alpha\beta_V}{4s_W^2 m_H}\right)\left[3M_V^2 - m_H^2 + \frac{m_H^4}{4M_V^2} + 4(d_{VV})^2\left\{3M_V^2 - 2m_H^2 + \frac{m_H^4}{2M_V^2}\right\}\right. \\ &\left. - 6d_{VV}(m_H^2 - 2M_V^2) + 2(\bar{d}_{VV})^2(m_H^2 - 4M_Z^2)\frac{m_H^2}{M_V^2}\right] ,\end{aligned} \tag{12}$$

with $C_W = 1$, $C_Z = 1/(2c_W^2)$, $d_{WW} = d$ and $d_{ZZ} = dc_W^2 + d_B s_W^2$.

For $M_V < m_H < 2M_V$, we have computed the Higgs decay width with one gauge boson being virtual and decaying into lepton and quark pairs. The expressions are

$$\Gamma(H \to W^*W) = \frac{3\alpha^2 m_H}{32\pi s_W^4}\left[D_{SM}(x) + dD_1(x) + 8d^2 D_2(x) + 8\bar{d}^2 D_3\right] \quad , \tag{13}$$

$$\begin{aligned}\Gamma(H \to Z^*Z) &= \frac{\alpha^2 m_H}{128\pi s_W^4 c_W^4}\left(7 - \frac{40s_W^2}{3} + \frac{160s_W^4}{9}\right)[D_{SM}(x) + (d_{ZZ})D_1(x) \\ &+ 8(d_{ZZ})^2 D_2(x) + 8(\bar{d}_{ZZ})^2 D_3(x)] \quad ,\end{aligned} \tag{14}$$

where

$$\begin{aligned}D_{SM}(x) &= \frac{3(20x^2 - 8x + 1)}{\sqrt{4x-1}} cos^{-1}\left(\frac{3x-1}{2x^{3/2}}\right) \\ &- (1-x)\left(\frac{47x}{2} - \frac{13}{2} + \frac{1}{x}\right) - 3(2x^2 - 3x + \frac{1}{2})lnx \quad ,\end{aligned} \tag{15}$$

$$\begin{aligned}D_1(x) &= \frac{24(14x^2 - 8x + 1)}{\sqrt{4x-1}} cos^{-1}\left(\frac{3x-1}{2x^{3/2}}\right) \\ &+ 12(x-1)(9x-5) - 12(2x^2 - 6x + 1)lnx \quad ,\end{aligned} \tag{16}$$

$$\begin{aligned}D_2(x) &= \frac{54x^3 - 40x^2 + 11x - 1}{x\sqrt{4x-1}} cos^{-1}\left(\frac{3x-1}{2x^{3/2}}\right) \\ &+ \frac{(x-1)}{6}(89x - 82 + \frac{17}{x}) - (3x^2 - 15x + \frac{9}{2} - \frac{1}{2x})lnx \quad ,\end{aligned} \tag{17}$$

$$D_3(x) = \frac{-28x^2+11x-1)}{x\sqrt{4x-1}} cos^{-1}\left(\frac{3x-1}{2x^{3/2}}\right) - \frac{x^2}{6} - \frac{21x}{2} + \frac{27}{2} - \frac{17}{6x} + \frac{(6x^2-9x+1)}{2x} lnx \quad , \tag{18}$$

and $x = (M_V/m_H)^2$ with $M_V = M_W$ or M_Z. These results are useful for $90GeV \lesssim m_H \lesssim 140GeV$. Finally we quote the $H \to b\bar{b}$ decay width, which is purely standard and particularly important if $m_H < 140GeV$. It is given by

$$\Gamma(H \to b\bar{b}) = 3\frac{\sqrt{2}G_F m_b^2}{8\pi}\beta_b^3 m_H \quad , \tag{19}$$

with $\beta_b = \sqrt{1-4m_b^2/m_H^2}$.

In Figs. 3a,b the ratios $\Gamma(H \to \gamma\gamma)/\Gamma(H \to b\bar{b})$ and $\Gamma(H \to \gamma Z)/\Gamma(H \to b\bar{b})$ are plotted versus m_H for a given value of d or $\bar{d}$. The case of d_B or $\bar{d}_B$ can be obtained by the respective replacements $d \to d_B c_W^2/s_W^2$ for the $\gamma\gamma$ amplitude and of $d \to d_B$ for the γZ one. The m_H and d dependences of the $\gamma\gamma/b\bar{b}$ ratio are obviously similar to the ones of the production cross section $\sigma(\gamma\gamma \to H)$. The ratios $\gamma Z/b\bar{b}$ and $\gamma\gamma/\gamma Z$ have independent features that may help disentangling the various couplings. They can also be seen from the ratio shown in Fig.3c.

The sensitivity of the $WW/b\bar{b}$ and $ZZ/b\bar{b}$ ratios is much weaker as expected from the occurrence of tree level SM contributions. Because of this these ratios are only useful for $d \gtrsim 0.1$. The ratios $\gamma\gamma/WW$ and $\gamma\gamma/ZZ$ are shown in Figs.3d,e and present the same features as the ratio $\gamma\gamma/b\bar{b}$. They can however be useful in the range of m_H where the WW, ZZ modes are dominant.

Finally we discuss the ratios WW/ZZ and $\gamma\gamma/\gamma Z$ for a given value of m_H (chosen as $0.2TeV$ in the illustrations made in Fig.4a,b), versus the coupling constant values of the four operators. This shows very explicitly how these ratios can be used for disentangling the various operators. They have to be taken in a complementary way to the $\sigma(\gamma\gamma \to H)$ measurement. As in the $WW/b\bar{b}$ case, the WW/ZZ ratio is only useful for $d \gtrsim 0.1$, while $\gamma\gamma/\gamma Z$ ratio allows for disentangling d values down to 10^{-3} or even less. The corresponding sensitivity limit for d_B, $\bar{d}_B$ should then be lying at the level of a few times 10^{-4}.

4 Final discussion

At a linear e^+e^- collider the process $\gamma\gamma \to H$ is a very efficient way to produce and study the Higgs boson. We showed that the sensitivity limits on the NP couplings are at the 10^{-3} level. Using unitarity relations in [11, 12, 5] we find and that this implies that new physics scales are in the range of 30 to 200 TeV, depending on the nature of the NP operator.

In more detail, we have studied the behaviour of $\sigma(\gamma\gamma \to H)$ versus m_H for the four NP operators which are the candidates to describe residual NP effects in the Higgs sector.

Ways to disentangle the effects of these operators have been considered. We have found that this can be achieved by looking at the Higgs branching ratios into WW, ZZ, $\gamma\gamma$, γZ, which react rather differently to the presence of each of these operators. This is illustrated with the ratios of these channels to the $b\bar{b}$ one which is unaffected by this kind of NP. Most spectacular for the disentangling of the various operators seem to be the ratios WW/ZZ and $\gamma\gamma/\gamma Z$. The first one, which is applicable in the intermediate and high Higgs mass range, allows to disentangle $\mathcal{O}_{UB}$ from $\mathcal{O}_{UW}$ down to values of the order of 10^{-1}, whereas the second one, applicable in the light Higgs case, is sensitive to couplings down to the 10^{-3} level or less.

The identification of CP-violating terms is not directly possible except for the remark that, contrarily to the CP-conserving terms, there can be no intereference with the tree level SM contributions. Thus a CP violating interaction cannot lower the value of the widths through a destructive intereference. A direct identification of CP violation requires either an analysis of the W or Z spin density matrix through their fermionic decay distributions [13, 14], or the observation of a suitable asymmetry with linearly polarized photon beams [15].

References

[1] I.Ginzburg et al, Nucl. Instrum. Methods **205**(1983)47; **219**(1984)5.

[2] G.J. Gounaris, J. Layssac and F.M. Renard, Z. Phys. **C65** (254) 1995.

[3] A. De Rújula, M.B. Gavela, P. Hernandez and E. Masso, Nucl. Phys. **B384** (1992) 3.

[4] K. Hagiwara, S. Ishihara, R. Szalapski and D. Zeppenfeld, Phys. Lett. **B283** (1992) 353 and Phys. Rev. **D48** (1993) 2182.

[5] G.J. Gounaris, F.M. Renard and G. Tsirigoti, preprint CERN-TH/95-42(1995), Phys. Letters B. (in press).

[6] G.J. Gounaris, F.M. Renard and C. Verzegnassi, Preprint PM/94-44 and THES-TP 95/01, hep-ph/9501362n to appear in Phys. Rev. D.

[7] G.J. Gounaris and F.M. Renard, Phys. Lett. **B326** (1994) 131 .

[8] G.J. Gounaris, J. Layssac and F.M. Renard, Montpellier and Thessaloniki preprint PM/95-11 and THES-TP 95/06.

[9] L. Bergström and G. Hulth, Nucl. Phys. **B259** (1985) 137; J. Gunion, H. Haber, G. Kane and S. Dawson, The Higgs Hunter's guide, Addison-Wesley, Reading 1990; B.A. Kniehl, Phys. Rep. **C240** (1994) 211.

[10] F. Abe *et.al.*, The CDF Collaboration, Phys. Rev. Lett. **73** (1994) [225; Phys. Rev. **D50** (1994) 2966; FERMILAB-PUB-95/022-E. S. Abachi *et.al.*, The D0 Collaboration, FERMILAB-PUB-95/028-E

[11] G.J. Gounaris, J. Layssac and F.M. Renard, Phys. Lett. **B332** (1994) 146 .

[12] G.J. Gounaris, J. Layssac, J.E. Paschalis and F.M. Renard, Montpellier preprint PM/94-28, to appear in Z. Phys.

[13] G.J. Gounaris, F.M. Renard and D. Schildknecht, Phys. Lett. **B263** (1993) 143 .

[14] G.J. Gounaris, F.M. Renard and N.D. Vlachos, Montpellier and Thessaloniki preprint THES-TP 95-08.

[15] M. Krämer, J. Kühn, M.L. Stong and P.M. Zerwas, Z. Phys. **C64** (1994) 21.

Figure Captions

Fig.1 Cross sections for Higgs production in $\gamma\gamma$ collisions from laser backscattering at a 0.5 TeV (a), 1 TeV (b), 2 TeV (c) e^+e^- linear collider. Standard prediction (solid line), with $d = +0.01$ (long dashed), $d = -0.01$ (dashed - circles), $d = +0.005$ (short dashed), $d = -0.005$ (dashed), $d = +0.001$ (dashed - stars), and $d = -0.001$ (dashed - boxes). The expected number of events per year for an integrated luminosity of $20fb^{-1}$, $80fb^{-1}$, $320fb^{-1}$ is also indicated.

Fig.2 Cross sections for Higgs production in $\gamma\gamma$ collisions from laser backscattering at a 0.5 TeV (a), 1 TeV (b), 2 TeV (c) e^+e^- linear collider. Standard prediction (solid line), with $\bar{d} = 0.01$ (long dashed), $\bar{d} = 0.001$ (short dashed), $\bar{d} = 0.005$ (dashed). The expected number of events per year for an integrated luminosity of $20fb^{-1}$, $80fb^{-1}$, $320fb^{-1}$ is also indicated.

Fig.3 Ratios of Higgs decay widths versus m_H, $\Gamma(H \to \gamma\gamma)/\Gamma(H \to b\bar{b})$ (a), $\Gamma(H \to \gamma Z)/\Gamma(H \to b\bar{b})$ (b), $\Gamma(H \to \gamma\gamma)/\Gamma(H \to \gamma Z)$ (c), $\Gamma(H \to \gamma\gamma)/\Gamma(H \to WW)$ (d), $\Gamma(H \to \gamma\gamma)/\Gamma(H \to ZZ)$ (e). Standard prediction (solid line), with $d = +0.01$ (short dashed), $d = -0.01$ (dashed), $\bar{d} = 0.01$ (long dashed).

Fig.4 Ratios of Higgs decay widths for $m_H = 0.2TeV$ versus coupling constant values, $\Gamma(H \to WW)/\Gamma(H \to ZZ)$ (a), $\Gamma(H \to \gamma\gamma)/\Gamma(H \to \gamma Z)$ (b). with $d > 0$ (solid), $d < 0$ (short dashed), $d_B > 0$ (dashed), $d_B < 0$ (long dashed), $\bar{d}$ (dashed-circles), $\bar{d}_B$ (dashed-stars).

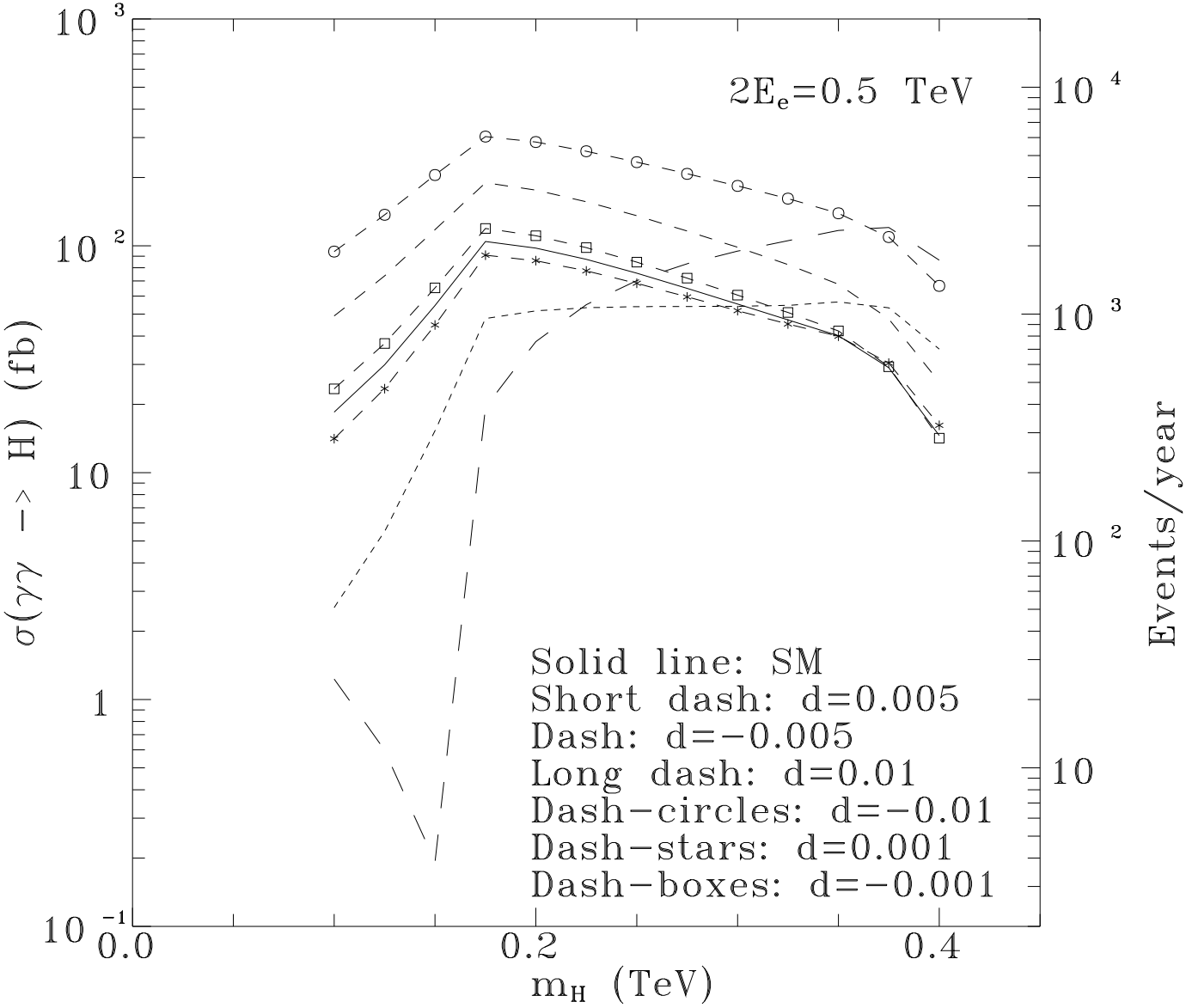
$2E_e$=0.5 TeV
Solid line: SM
Short dash: d=0.005
Dash: d=−0.005
Long dash: d=0.01
Dash−circles: d=−0.01
Dash−stars: d=0.001
Dash−boxes: d=−0.001
$\sigma(\gamma\gamma \rightarrow H)$ (fb)
Events/year
m_H (TeV)
10^3
10^2
10
1
10^{-1}
10^4
10^3
10^2
10
0.0
0.2
0.4

Fig 1a

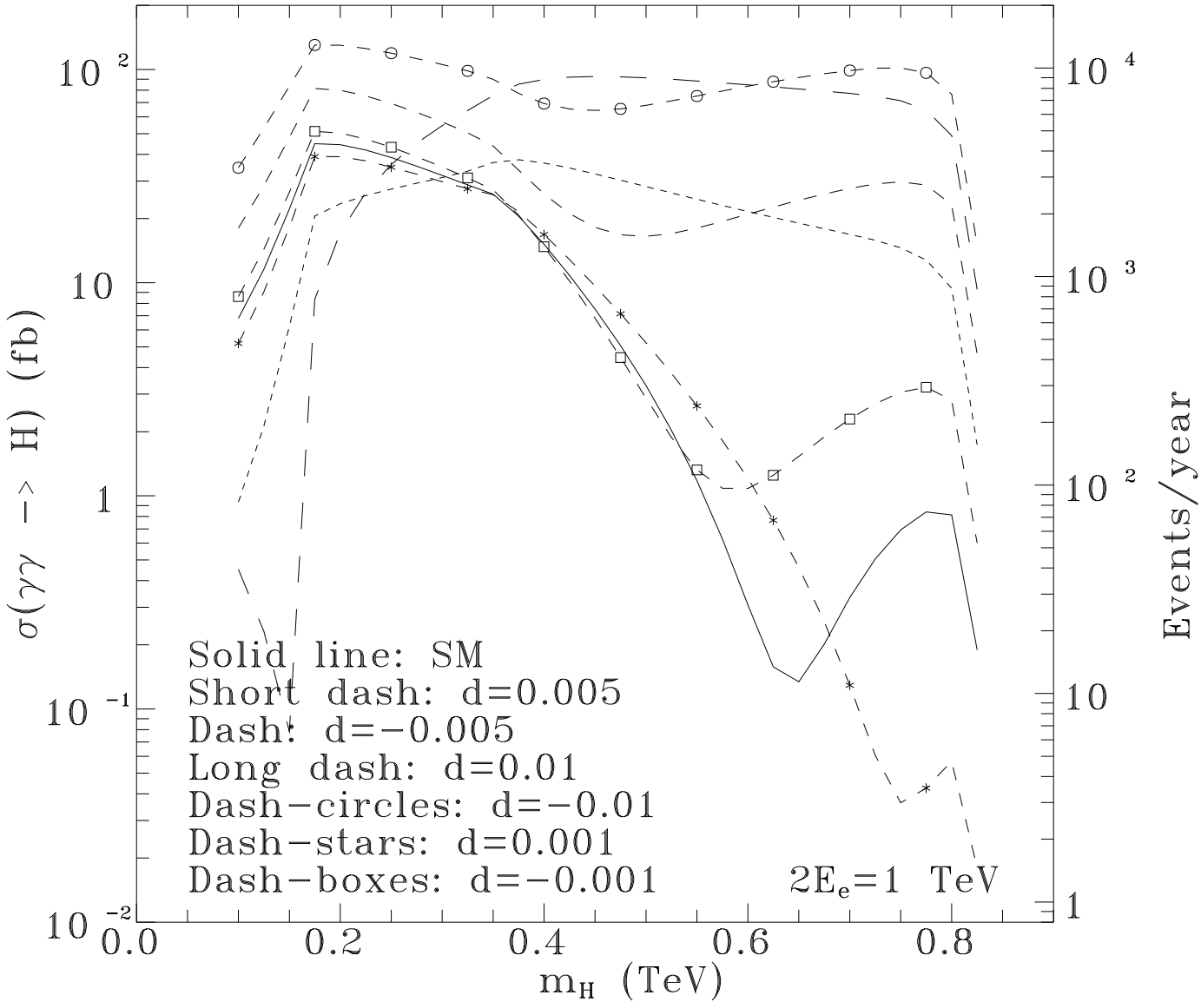
10^2
10
1
10^{-1}
10^{-2}
$\sigma(\gamma\gamma \rightarrow H)$ (fb)
0.0
0.2
0.4
0.6
0.8
m_H (TeV)
10^4
10^3
10^2
10
1
Events/year
Solid line: SM
Short dash: d=0.005
Dash: d=−0.005
Long dash: d=0.01
Dash−circles: d=−0.01
Dash−stars: d=0.001
Dash−boxes: d=−0.001
$2E_e$=1 TeV

Fig 1b

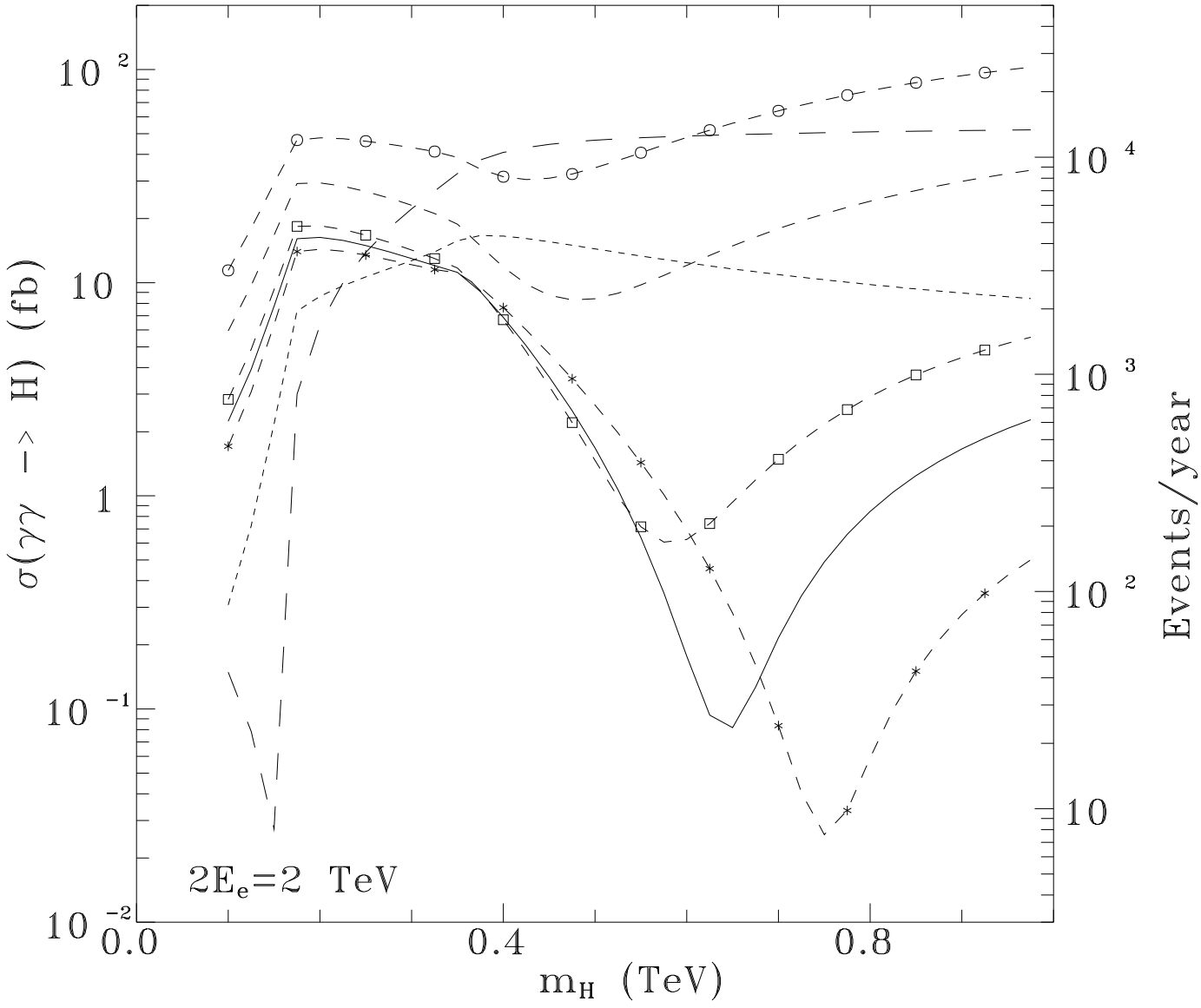
10^{2}
10
1
10^{-1}
10^{-2}
$\sigma(\gamma\gamma \rightarrow H)$ (fb)
10^{4}
10^{3}
10^{2}
10
Events/year
$2E_e$=2 TeV
0.0
0.4
0.8
m_H (TeV)

Fig 1c

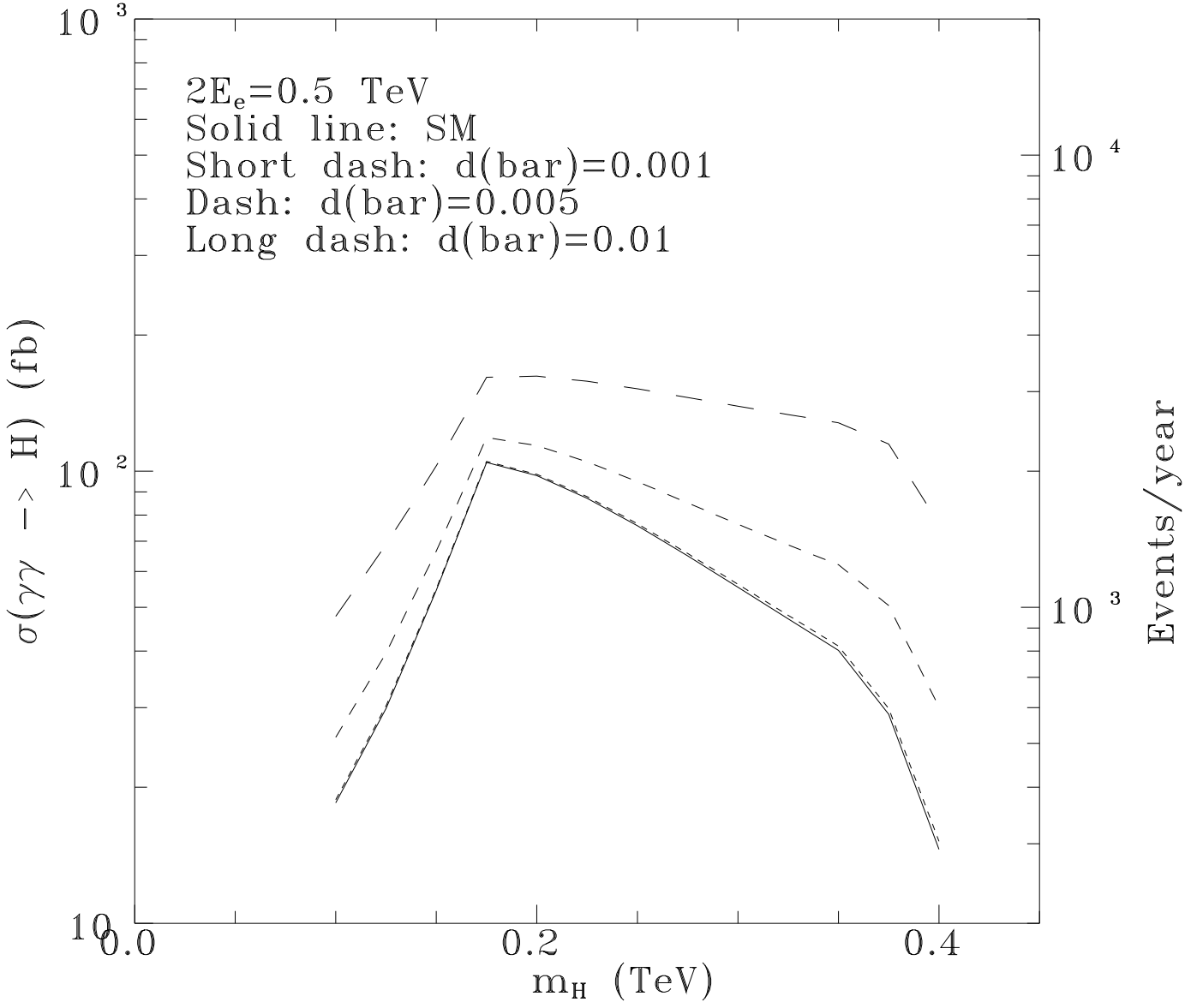
$2E_e$=0.5 TeV
Solid line: SM
Short dash: d(bar)=0.001
Dash: d(bar)=0.005
Long dash: d(bar)=0.01
10^3
10^2
10
0.0
0.2
0.4
m_H (TeV)
$\sigma(\gamma\gamma \rightarrow H)$ (fb)
10^4
10^3
Events/year

Fig 2a

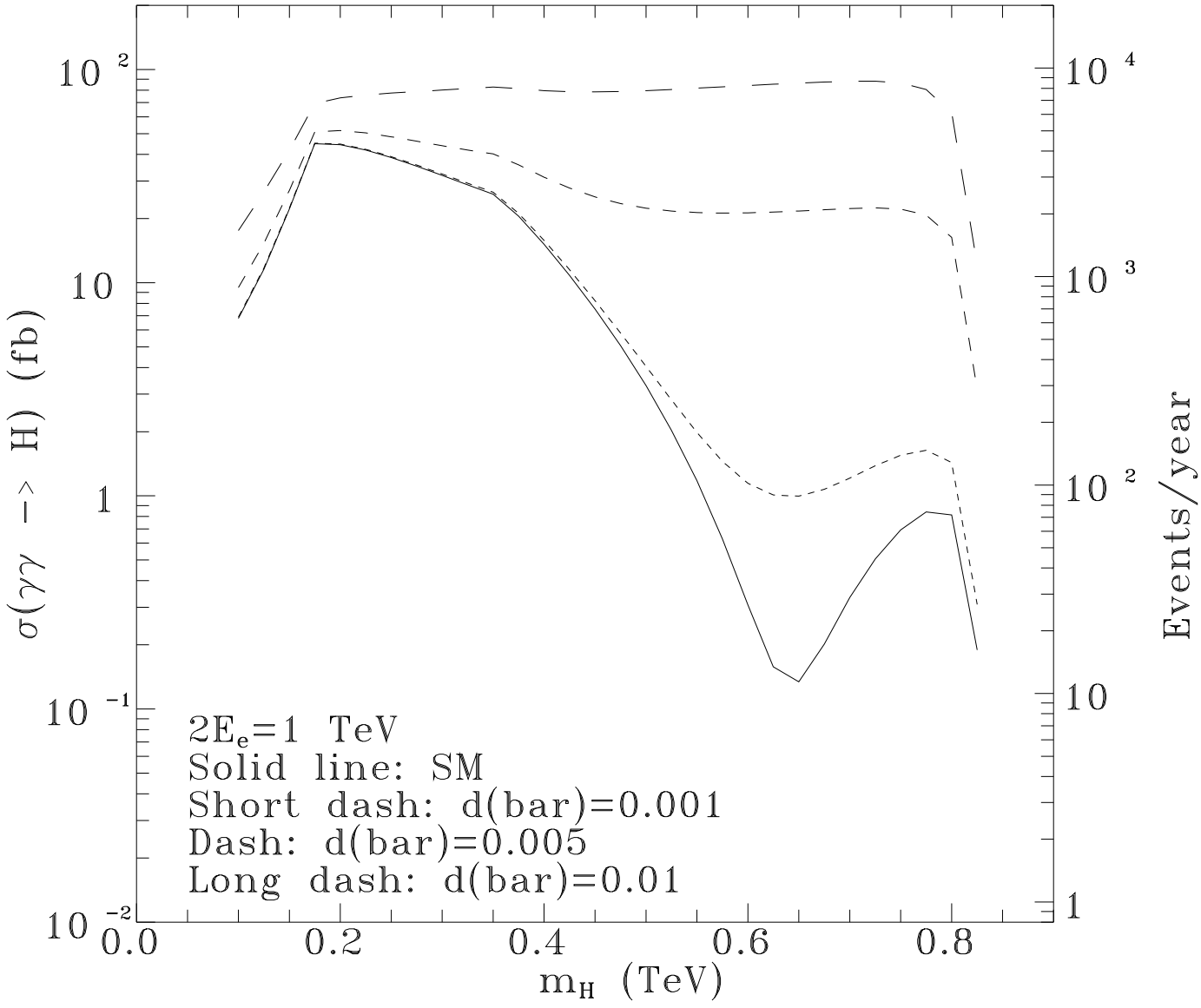
10^2
10
1
10^{-1}
10^{-2}
$\sigma(\gamma\gamma \rightarrow H)$ (fb)
10^4
10^3
10^2
10
1
Events/year
0.0
0.2
0.4
0.6
0.8
m_H (TeV)
$2E_e$=1 TeV
Solid line: SM
Short dash: d(bar)=0.001
Dash: d(bar)=0.005
Long dash: d(bar)=0.01

Fig 2b

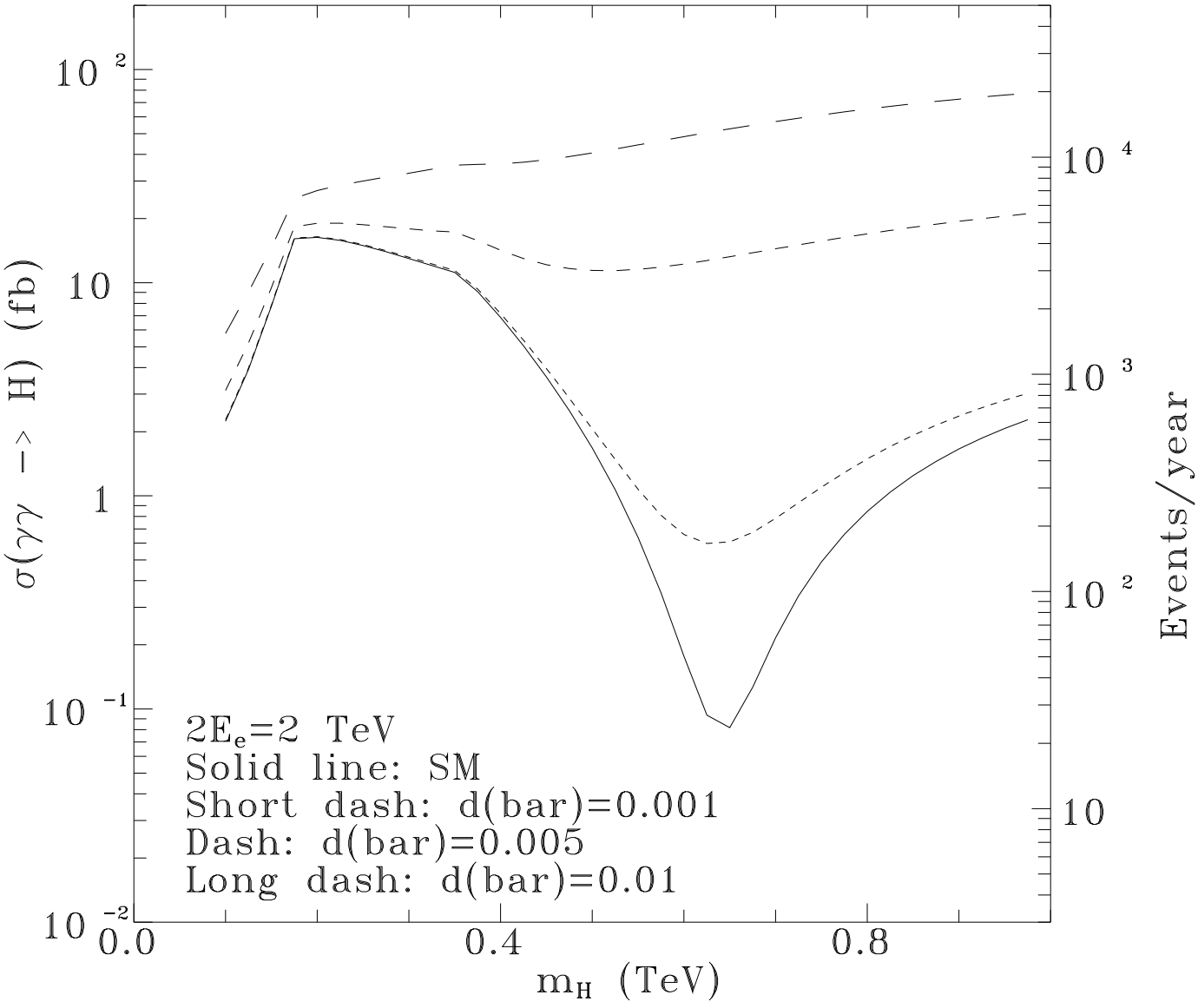
10^2
10
1
10^{-1}
10^{-2}
$\sigma(\gamma\gamma \rightarrow H)$ (fb)
10^4
10^3
10^2
10
Events/year
$2E_e$=2 TeV
Solid line: SM
Short dash: d(bar)=0.001
Dash: d(bar)=0.005
Long dash: d(bar)=0.01
0.0
0.4
0.8
m_H (TeV)

Fig 2c

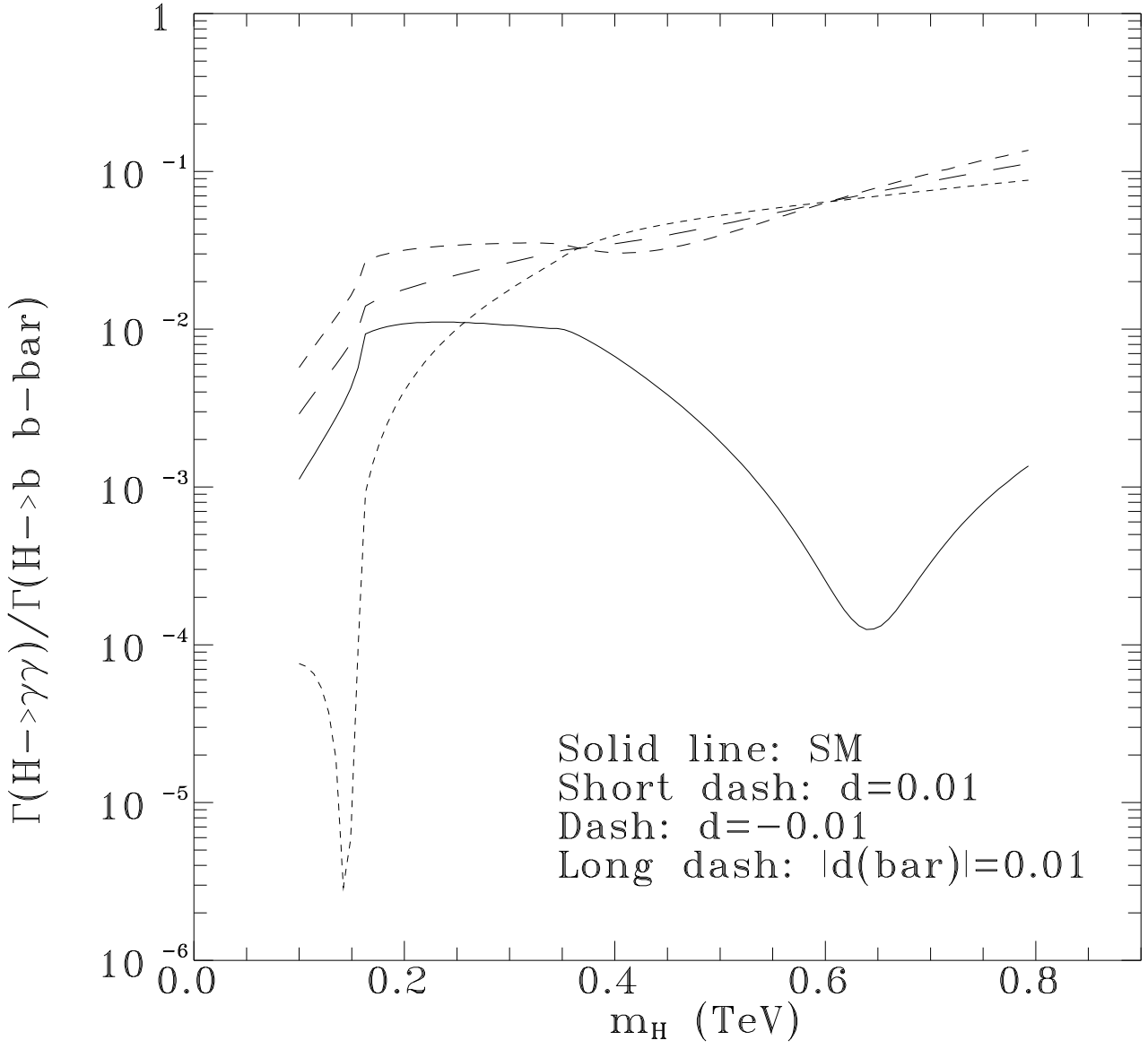
1
10 -1
10 -2
10 -3
10 -4
10 -5
10 -6
0.0
0.2
0.4
0.6
0.8
m_H (TeV)
Γ(H−>γγ)/Γ(H−>b b−bar)
Solid line: SM
Short dash: d=0.01
Dash: d=−0.01
Long dash: |d(bar)|=0.01

Fig 3a

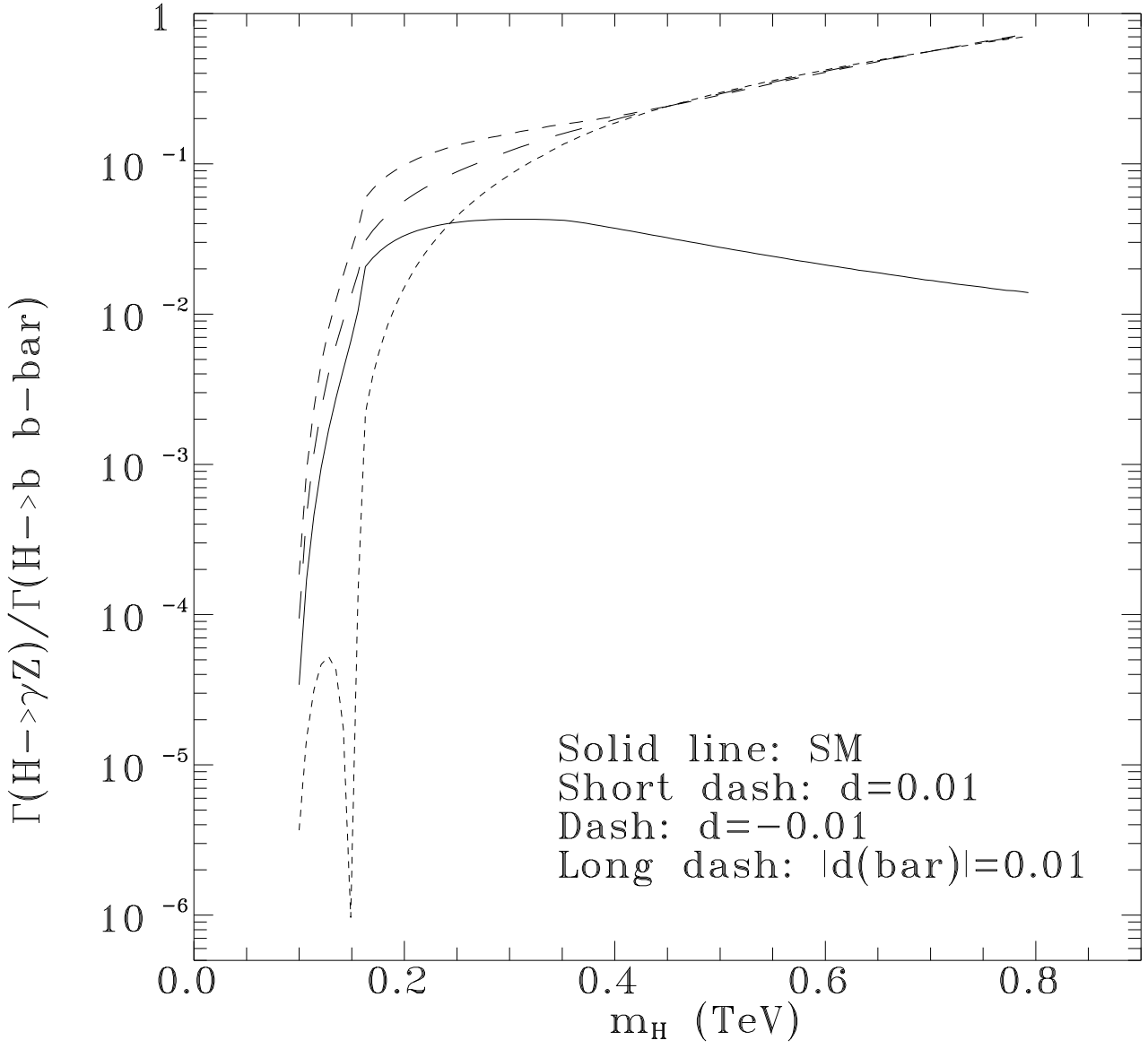
1
10 -1
10 -2
10 -3
10 -4
10 -5
10 -6
0.0
0.2
0.4
0.6
0.8
m_H (TeV)
Γ(H−>γZ)/Γ(H−>b b−bar)
Solid line: SM
Short dash: d=0.01
Dash: d=−0.01
Long dash: |d(bar)|=0.01

Fig 3b

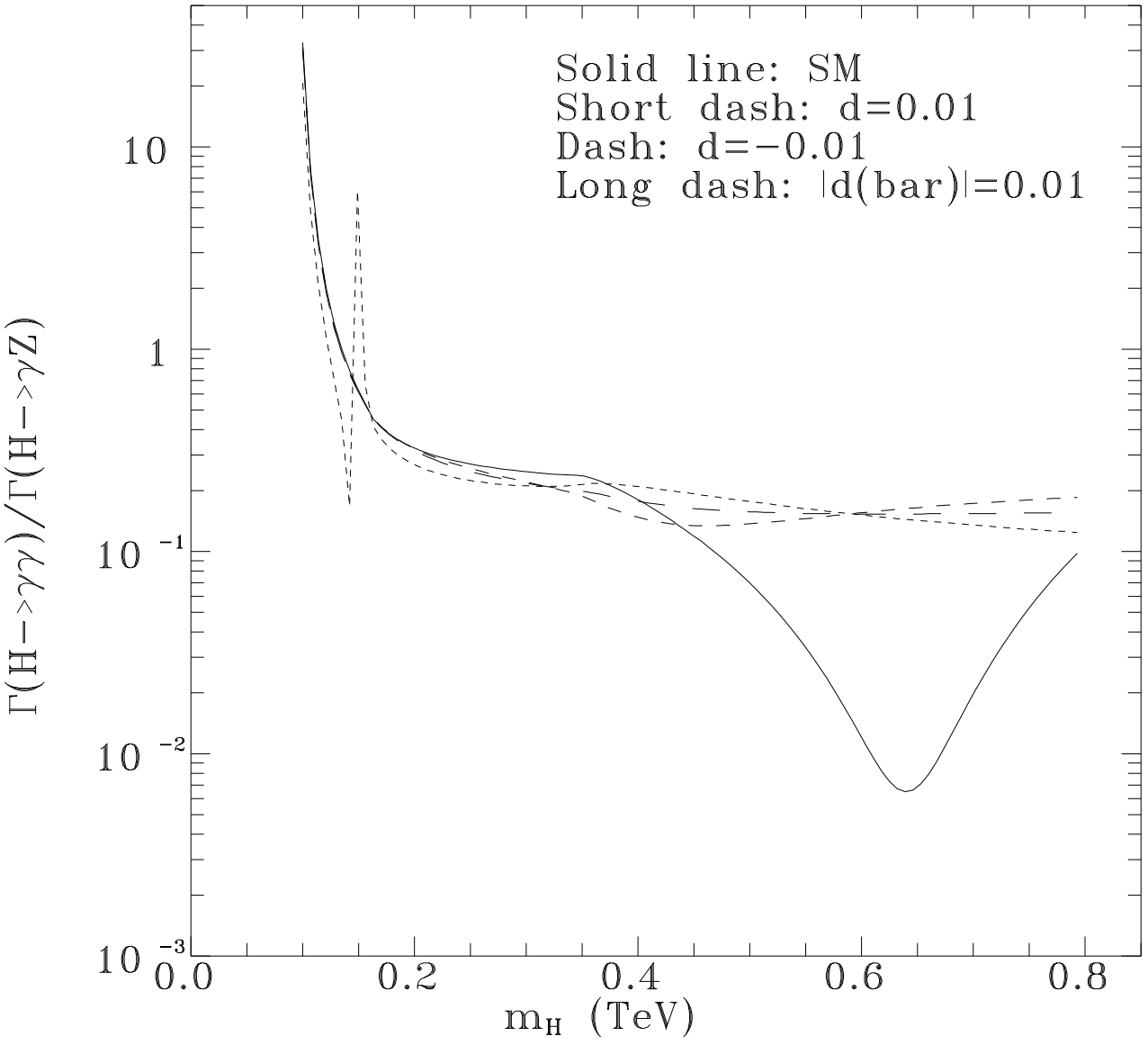
Solid line: SM
Short dash: d=0.01
Dash: d=−0.01
Long dash: |d(bar)|=0.01
Γ(H−>γγ)/Γ(H−>γZ)
10
1
10 -1
10 -2
10 -3
0.0
0.2
0.4
0.6
0.8
m_H (TeV)

Fig 3c

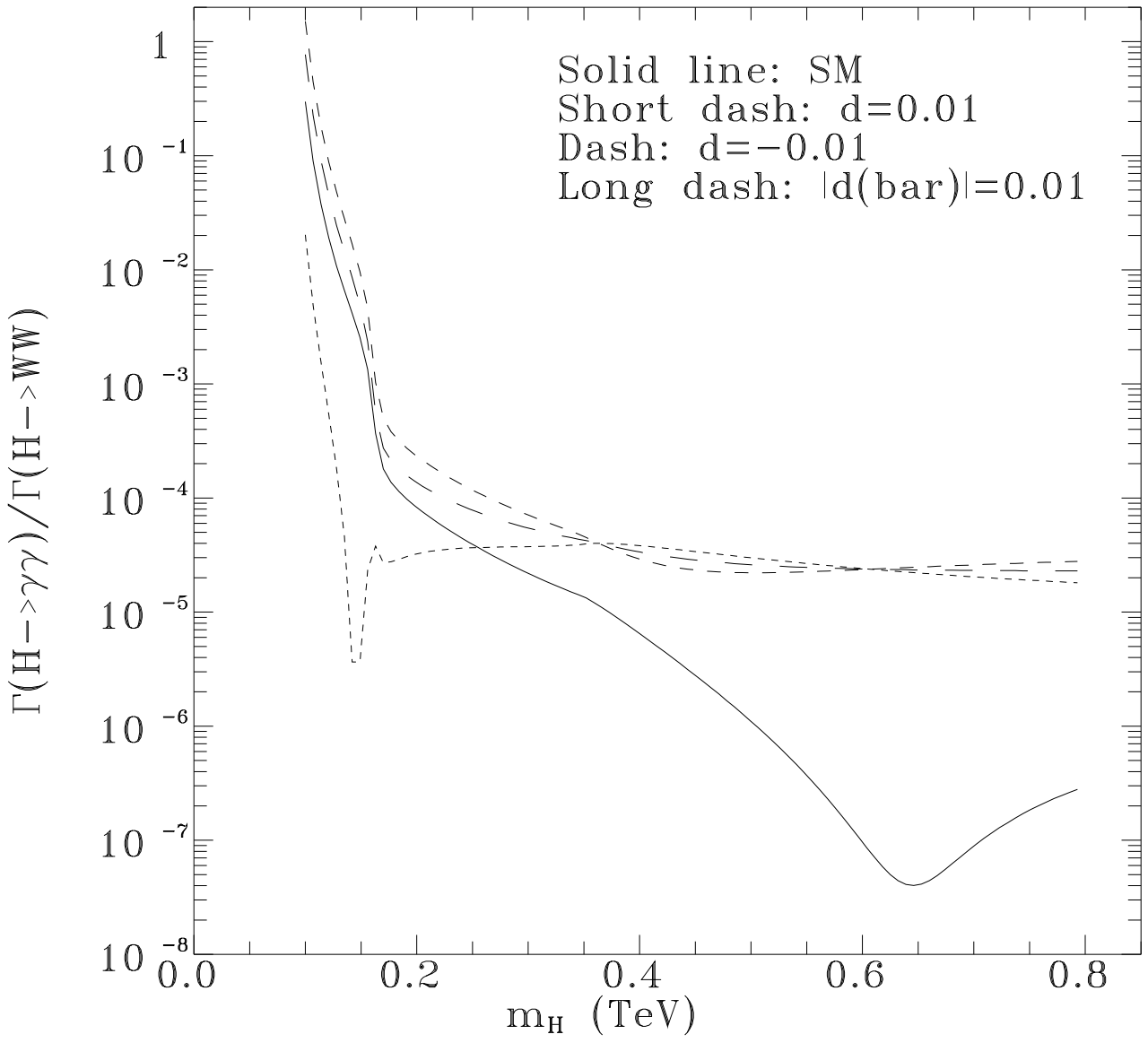
Solid line: SM
Short dash: d=0.01
Dash: d=−0.01
Long dash: |d(bar)|=0.01
Γ(H−>γγ)/Γ(H−>WW)
m_H (TeV)
1
10 −1
10 −2
10 −3
10 −4
10 −5
10 −6
10 −7
10 −8
0.0
0.2
0.4
0.6
0.8

Fig 3d

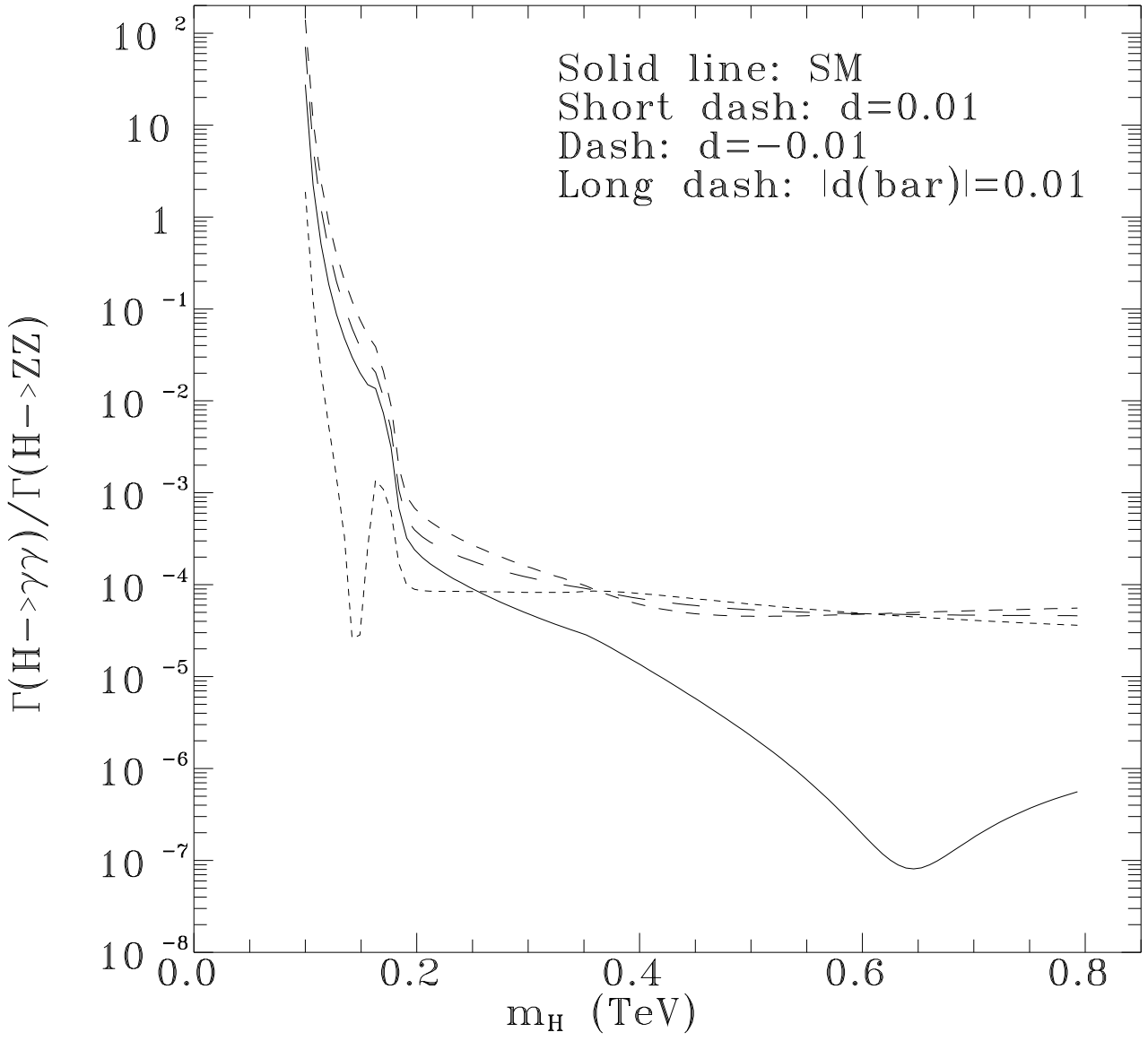
Solid line: SM
Short dash: d=0.01
Dash: d=−0.01
Long dash: |d(bar)|=0.01
Γ(H−>γγ)/Γ(H−>ZZ)
m_H (TeV)
10^2
10
1
10^-1
10^-2
10^-3
10^-4
10^-5
10^-6
10^-7
10^-8
0.0
0.2
0.4
0.6
0.8

Fig 3e

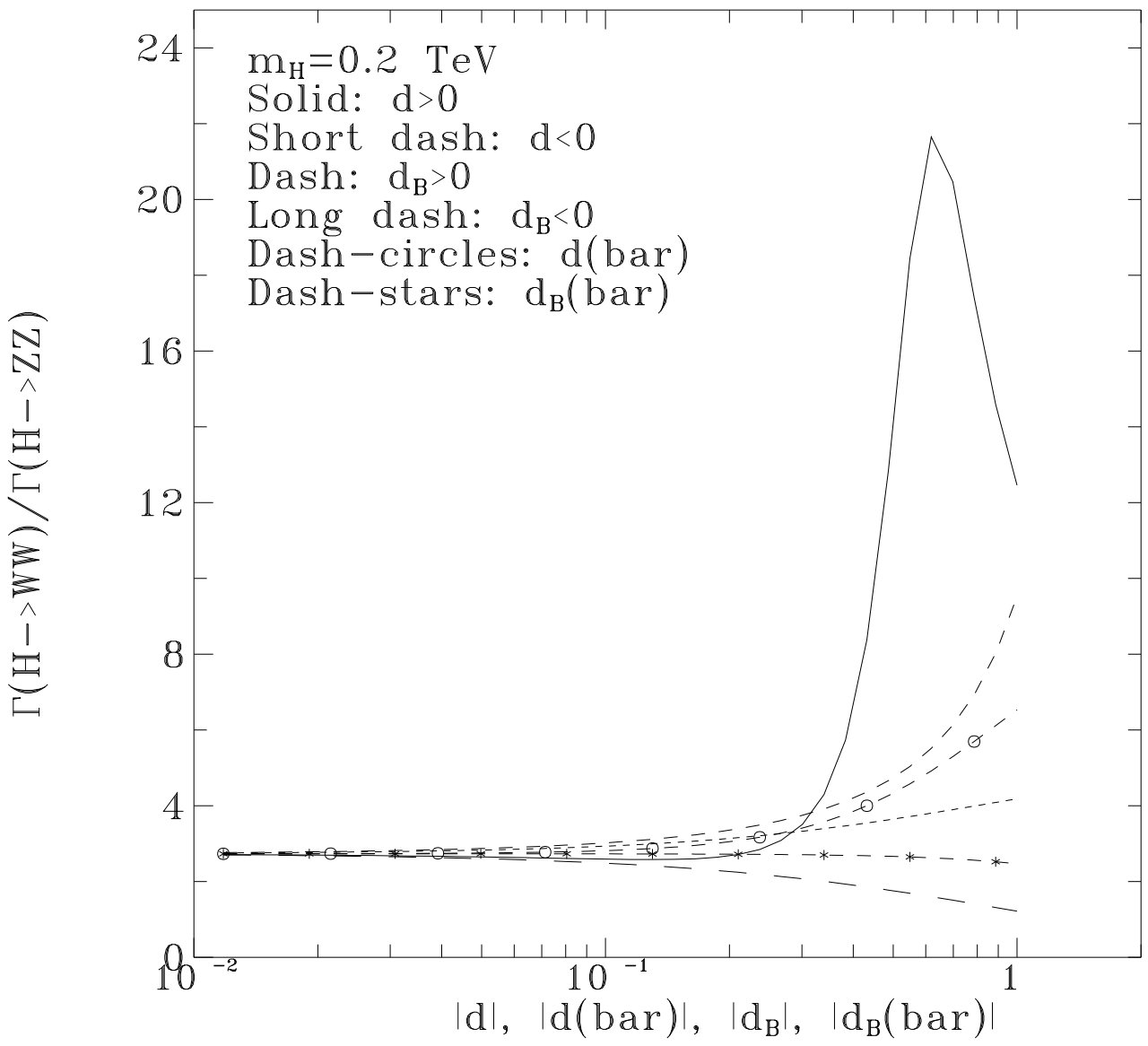
m_H=0.2 TeV
Solid: d>0
Short dash: d<0
Dash: d_B>0
Long dash: d_B<0
Dash−circles: d(bar)
Dash−stars: d_B(bar)
Γ(H−>WW)/Γ(H−>ZZ)
|d|, |d(bar)|, |d_B|, |d_B(bar)|
0
4
8
12
16
20
24
10^{-2}
10^{-1}
1

Fig 4a

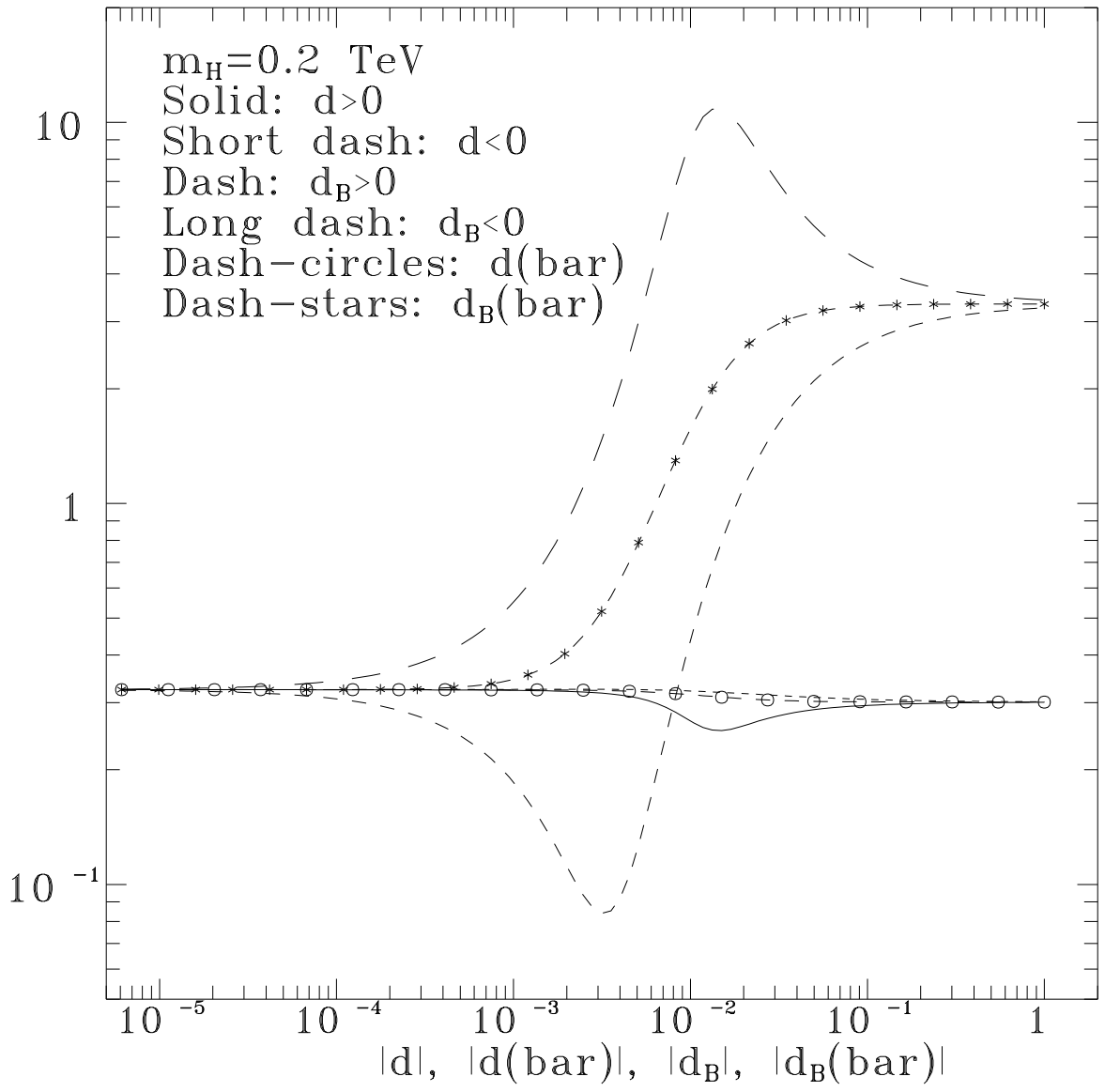
m_H=0.2 TeV
Solid: d>0
Short dash: d<0
Dash: d_B>0
Long dash: d_B<0
Dash−circles: d(bar)
Dash−stars: d_B(bar)
10
1
10^{-1}
10^{-5}
10^{-4}
10^{-3}
10^{-2}
10^{-1}
1
|d|, |d(bar)|, $|d_B|$, $|d_B$(bar)|
$\Gamma(H->\gamma\gamma)/\Gamma(H->\gamma Z)$

Fig 4b